JOURNAL OF MATERIALS SCIENCE 24 (1989) 1252–1256

Friction and wear of rubber/epoxy composites

C. LHYMN, Y. LHYMN
YOON Technology, 3320 Buffalo Street, Erie, Pennsylvania 16510, USA

The sliding wear rate and frictional coefficient of epoxy/rubber or epoxy/rubber/aluminium oxide composites were measured against themselves as a wear rate. The observed wear rate–sliding velocity data appear to be explicable by a recently proposed fatigue-shear model based on damage accumulation physics. The proposed equation seems to explain both dry and wet friction (water lubricant) environments. The microstructural features of a worn surface were examined using a scanning electron microscope (SEM) and related to the measured tribological data.

1. Introduction

The wear behaviour is very complex. The complexity of wear phenomena can be seen, for example, by the numerous wear mechanisms proposed in the past [1–3]. Microstructurally, the phenomena such as micro-cracking, plowing, microcutting, plastic deformation, and fracture have been cited as wear-related material failure [4]. The failure processes cited above are very much related to the crack propagation phenomenon either in a brittle or ductile mode. When the asperity/asperity contact temperature becomes very high, wear loss can take place by solid–gas phase transformation, i.e. evaporation. In such use, the contribution of crack propagation to wear is minor. In this report, an analytical framework on wear by evaporation will be provided and experimental data supporting the proposed analysis will be provided for epoxy matrix/ rubber particle composites.

2. Experimental procedure

The rubber particles used for fabricating epoxy/rubber composites are shredded/powdered waste tyre rubber; a typical histogram for size distribution is shown in Fig. 1. The appropriately weighed epoxy/rubber mixture was thoroughly mixed for about 15 min and then poured into a mould for overnight curing. The size of the aluminium oxide particles added was about 0.05 μm.

The specimens for the sliding wear test were of square bar geometry, $3 \times 3\,mm^2$ contact area and about 12 mm long, and were prepared by cutting/grinding procedures. The contact surface was given a final grinding treatment with a grade 600 emery paper prior to desiccating. Two kinds of sliding wear tester were employed: pin-on-disc tester and a pin-on-table reciprocating unit [5, 6]. In the pin-on-disc type, the countermate disc was itself ground with a grade 600 emery paper and the speed was controlled by the control box attached to the electric motor as detailed before [5]. The test environment was air or water. It was found that a test duration of 30 min was sufficient to obtain a steady state wear rate. In the pin-on-table unit, the wear mate was grade 400 emery paper mounted on the reciprocating sliding table. After each stroke, the sliding table was moved laterally so as to expose a fresh wear track to the specimen and the reciprocating motion was powered by an air motor [6]. For both tests the specific wear rate was determined by the following equation

$$W_S = \frac{\Delta m}{\varrho F_N S} = \frac{\Delta V}{F_N S} \quad (1)$$

where Δm is the weight loss, ϱ the density, F_N the normal load, S the sliding distance, and ΔV the volume loss. The weight loss was measured with an electronic balance with 0.01 mg readability. The coefficient of friction, μ, was determined from the ratio

$$\mu = \frac{F_f}{F_N} \quad (2)$$

with F_f, the frictional force, obtained from the strain-gauge output. Detailed schematic drawings of the pin-on-disc and pin-on-table testers are shown in Fig. 2.

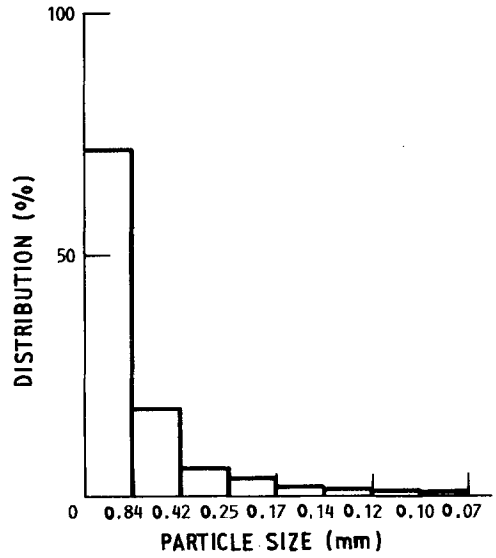

Figure 1 Size distribution of waste rubber particles.

0022–2461/89 $03.00 + .12

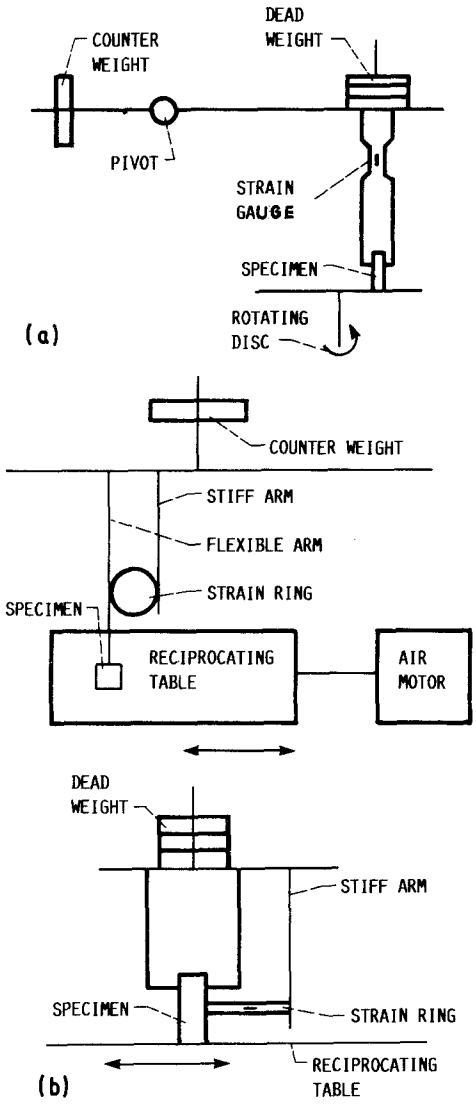

Figure 2 (a) Schematic drawing of pin-on-disc tester. (b) Schematic drawing of pin-on-table tester.

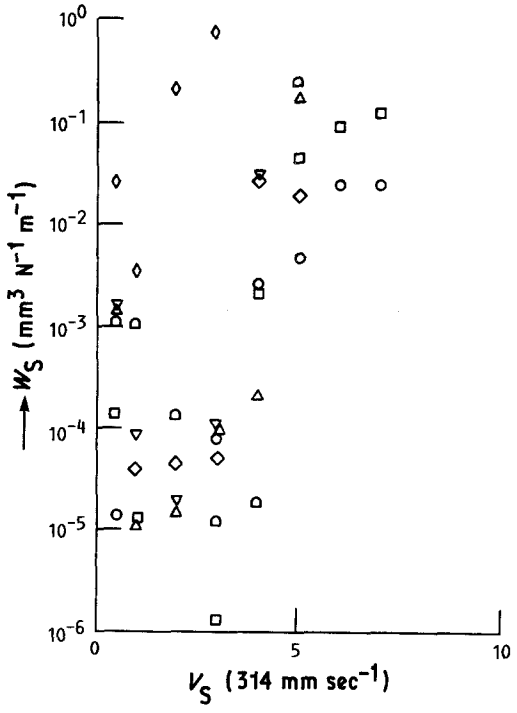

Figure 3 Specific wear rate plotted against sliding velocity for epoxy/rubber composites slid against themselves in air under 180 g load. Rubber content (wt %): (○) 0, (□) 10, (◇) 20, (△) 30, (▽) 40, (⌂) 50, (◇) 60.

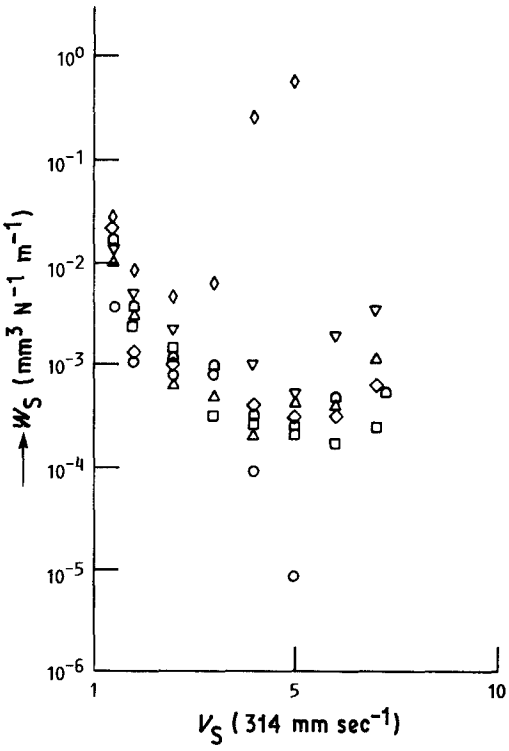

Figure 4 Same as Fig. 3, in water lubricant. For key, see Fig. 3.

The worn surface microstructures were examined by scanning electron microscopy.

3. Results and discussion

The specific wear rate–sliding velocity data for epoxy/rubber composites is shown in Figs 3 and 4 for air and water environments, respectively. Generally, the curves exhibit the presence of a minimum, though the wear rate of unfilled epoxy in water keeps decreasing with V_S within the range of V_S. Particularly noteworthy is an exponential rise of W_S with V_S at high velocities and such a trend is strikingly evident for testing in air. At low sliding velocities, W_S tends to decrease with increasing V_S. Apparently, the presence of water will reduce the effect of thermal heating at contact sites and this is most likely the reason for the reduced W_S rise with V_S for testing in water. Also, W_S tends to be relatively high for testing in water compared to testing in air in the low velocity range, probably due to the easy removal of wear debris and the effective abrasive action of debris particles between wear mates.

The frictional coefficient data corresponding to Figs 3 and 4 are shown in Figs 5 and 6. In a water environment, μ generally tends to remain constant with V_S. In an air environment, the μ–V_S data tend to reveal the presence of a maximum within the limit of

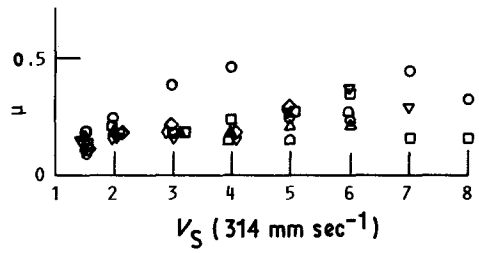

Figure 5 The coefficient of friction plotted against sliding velocity for Fig. 3 specimens. For key, see Fig. 3.

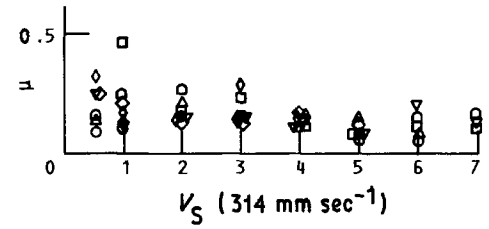

Figure 6 The coefficient of friction plotted against sliding velocity for Fig. 4 specimens. For key, see Fig. 3.

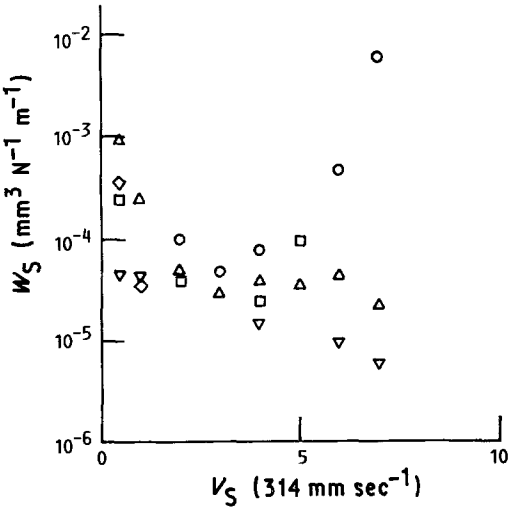

Figure 7 Specific wear rate plotted against sliding velocity for epoxy/rubber/aluminium oxide composites slid on themselves in air under 180 g load. Al_2O_3 content (wt %): (○) 30, (□) 20, (◇) 15, (△) 10, (▽) 0.

the specimen's structural irregularity. Such a trend exhibiting a maximum has been explained by a damage accumulation model of friction [5] and also by the energy balance model of friction in its expanded formulation [6].

When fine alumina particles are added, the W_S–V_S data generally exhibit a decreasing trend both in air and water lubricant, as shown in Figs 7 and 8. One exception, though, is the case of 70 wt % epoxy/

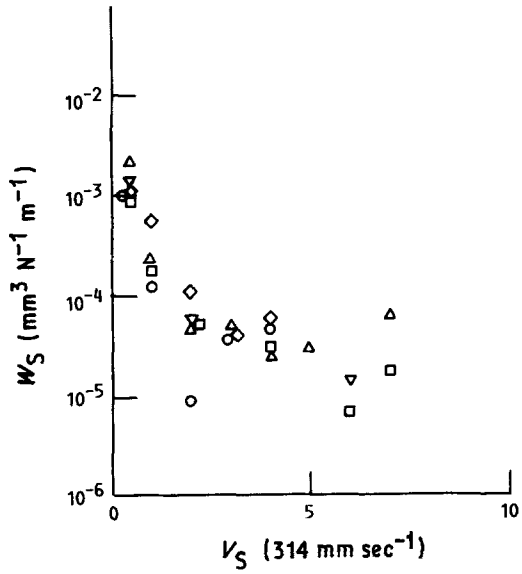

Figure 8 Same as Fig. 7, in water lubricant. Al_2O_3 (wt %): (○) 30, (□) 20, (◇) 15, (△) 10, (▽) 5.

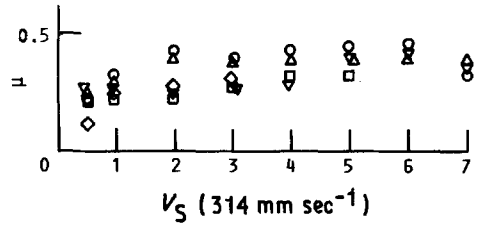

Figure 9 Coefficient of friction plotted against sliding velocity for Fig. 7 specimens. For key, see Fig. 8.

30 wt % Al_2O_3 composite in dry friction against itself which shows the presence of a minimum and this is probably due to the thermal heating effect. The coefficient of friction–sliding velocity data for Figs 7 and 8 are shown in Figs 9 and 10. Generally, the frictional coefficient in dry contact is higher than in wet contact and the dry frictional coefficient tends to rise with V_S, while the wet coefficient tends to remain constant or slightly decrease. For dry friction, somehow the presence of Al_2O_3 phase appears to withstand the thermal effect over the range of velocities tested, because μ initially rises with V_S and then falls when the thermal effect takes control of frictional phenomena [5]. For wet friction of epoxy/rubber/alumina composites, the preceding explanation does not seem to be applicable. In this case, the plowing aspect appears to contribute to friction significantly at low velocities. At high velocities the debris could be quickly removed and the fluid film thickness between mates will increase with V_S, thus reducing the effect of plowing action by trapped wear debris.

For two-body abrasion tests, wear and frictional data as a function of rubber (or alumina) content are shown in Figs 11 and 12 for epoxy/rubber and for epoxy/rubber/alumina composites, respectively. The wear rate increases with increasing rubber content for epoxy/rubber composites but for epoxy/rubber/alumina composites, respectively. The wear rate increases with increasing rubber content for epoxy/rubber composites but for epoxy/rubber/alumina composites, the wear rate–alumina content data exhibit the presence of a maximum (Fig. 12). The coefficient of friction data generally remain constant for both cases. The wear rate of rubber is higher than for epoxy and thus the wear loss increases with rubber, as seen in Fig. 11. When hard alumina particles are added, the wear rate will decrease with increasing alumina content and thus the competition between the rubber phase as the wear-increasing agent and the alumina as the wear-reducing agent will determine the resultant wear rate of the epoxy/rubber/alumina composite system (Fig. 12).

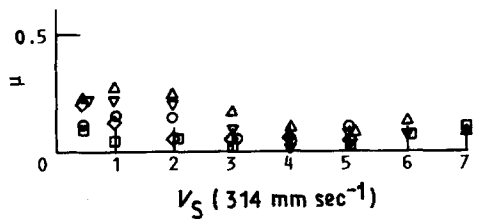

Figure 10 Coefficient of friction plotted against sliding velocity for Fig. 8 specimens. For key, see Fig. 8.

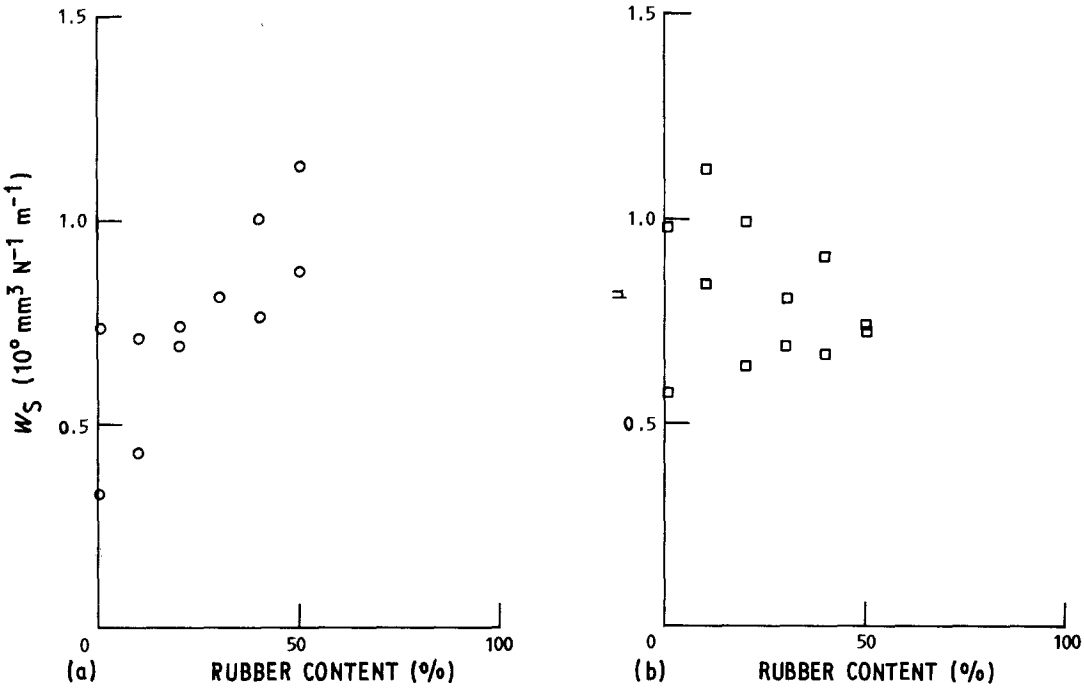

Figure 11 (a) Specific wear rate plotted against rubber content for epoxy/rubber composites slid on grit number 400 emery paper in air under 185 g load. (b) Frictional coefficient plotted against rubber content for specimens in (a).

A worn surface microstructure of 70 wt % epoxy/30 wt % rubber composite is shown in Fig. 13. Powderized rubber and epoxy particles are seen, as well as cracks induced by sliding. Cracks are present both in rubber and epoxy phases as well as the epoxy/rubber interface. A worn surface micrograph of 70 wt % epoxy/20 wt % rubber/10 wt % alumina composite is shown in Fig. 14. Cracks are mostly visible in the rubber or epoxy areas. The worn surface structure of an unfilled neat epoxy resin reveals prolific microcracking and fine powder seemingly generated by thermomechanical disintegration, as shown in Fig. 15. A typical fracture surface of 50 wt % rubber composite reveals the presence of microvoids as shown in Fig. 16. This appears to be intrinsic to our moulding method employed.

A possible explanation for the rise of W_S at high sliding velocities is as follows. As derived before, the specific wear rate can be expressed by [7]

$$(W_S)_c = C_1 \frac{V_C}{V_S} \frac{\mu}{EH\varepsilon_f} \quad (3)$$

where $(W_S)_c$ is the specific wear rate due to the crack propagation mechanism, V_C the crack propagation velocity, V_S the sliding velocity, E Young's modulus, H the hardness, ε_f the failure strain, and C_1 is a parametric constant incorporating the effects of roughness, debris geometry, material constant, and system

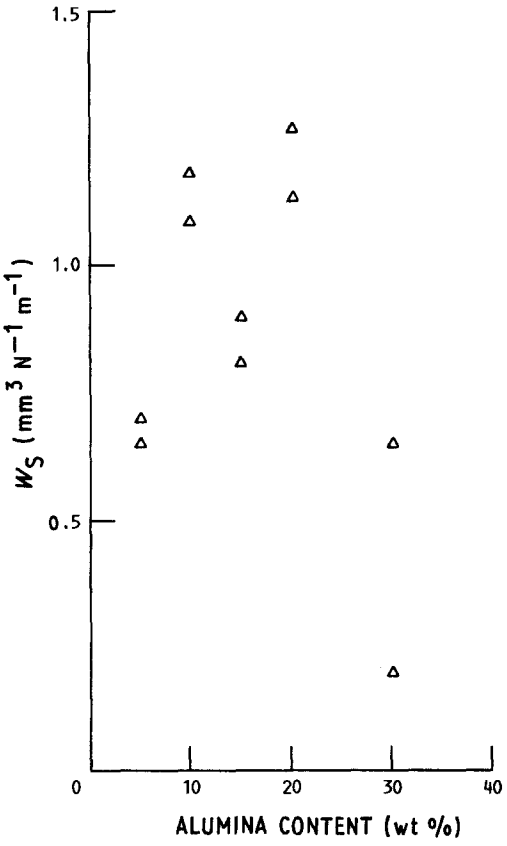

Figure 12 Specific wear rate plotted against alumina content for epoxy (70 wt %)/rubber/alumina composites slid on grit number 400 emery paper in air under a 180 g load.

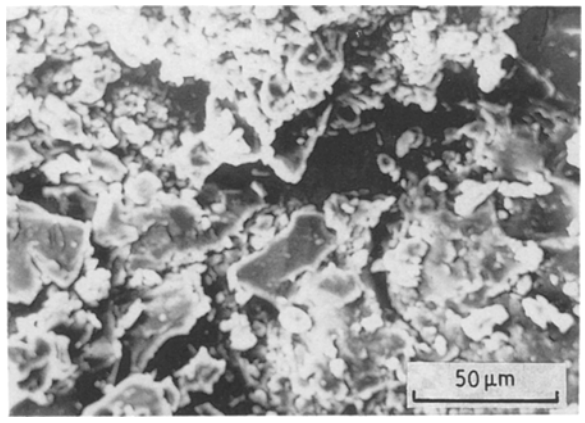

Figure 13 Scanning electron micrograph of 70 wt % epoxy/30 wt % rubber composite worn against itself in air under a 180 g load in a pin-on-disc unit.

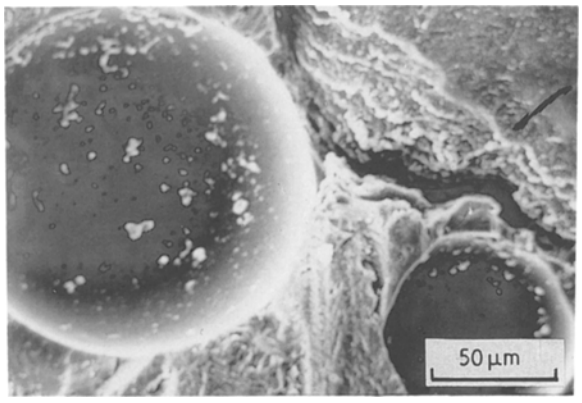

Figure 14 Scanning electron micrograph of 70 wt % % epoxy/20 wt % rubber/10 wt % alumina composite worn against itself in air under a 180 g load in a pin-on-disc unit.

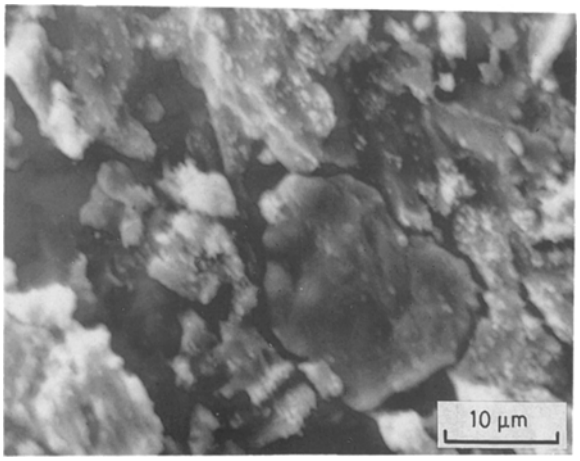

Figure 15 Scanning electron micrograph of unfilled epoxy worn against itself in air under a 180 g load in a pin-on-disc unit.

geometry, and surface adhesional coefficient. W_S can rise at high V_S when the following phenomena take place: (1) strength degradation (decrease of E and H); (2) thermal activation of V_C (increase of V_C); (3) disintegration due to interfacial reactions. Interfacial reactions, such as vapourization, result in wear loss and the specific wear rate due to the interfacial reactions is denoted by $(W_S)_r$. Then, the total wear rate is given by

$$W_S = (W_S)_c + (W_S)_r \quad (4)$$

Briefly, $(W_S)_r$ is rate controlled by adsorption or diffusion and thus thermally activated, i.e. $(W_S)_r$ rises as T increases [5]. It has been implicitly assumed that T is proportional to V_S in the preceding analysis.

For our epoxy/rubber/(alumina) composites, the increase in W_S at high V_S appears to be the result of strength degradation and thermal activation of V_C. The role of interfacial reactions in this system seems to be less significant.

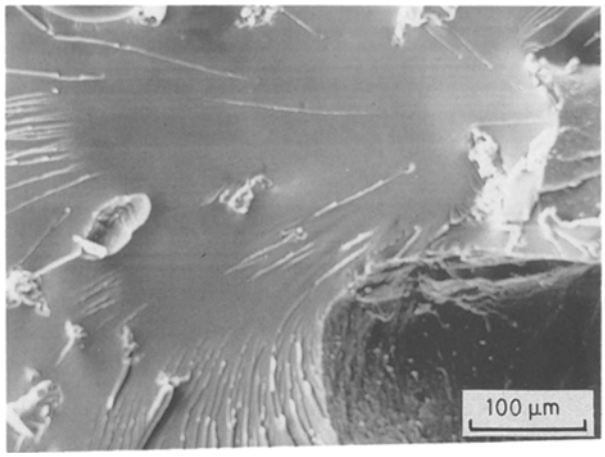

Figure 16 Scanning electron micrograph of 50 wt % epoxy/50 wt % rubber fracture surface.

4. Conclusions

1. The specific wear rate decreases with increase in sliding velocity at low velocities. This simply reflects the results of the wear model developed from the fatigue-shear concepts when the thermal effect is not significant.

2. When the contact temperature rise becomes significant at high sliding velocities, the specific wear rate increases with increasing sliding velocity. This is the result of thermally activated processes and the fatigue-shear model can explain this phenomenon. The increase in wear rate at high V_S is clearly evident for solid/solid contact as in epoxy/rubber (or epoxy/rubber/alumina) against itself.

3. As thermally activated processes, crack propagation and interfacial reactions have been considered.

4. The presence of water lubricant somewhat diminishes the effect of thermal activation.

Acknowledgement

The author acknowledges the help of Mr T. Reese for his work on mechanical data collection.

References

1. D. A. RIGNEY (ed.) "Fundamentals of Friction and Wear of Materials" (ASM, Metals Park, Ohio, 1981).
2. E. RIBINOWICZ, "Friction and Wear of Materials" (Wiley, New York, 1965).
3. I. V. KRAGELSKY, M. N. DOBYCHIN and V. S. KOMBALOV, "Friction and Wear-Calculation Methods" (Pergamon, Oxford, 1982).
4. K. FRIEDRICH (ed.) "Friction and Wear of Polymer Composites" (Elsevier, 1986).
5. C. LHYMN, *Adv. Polym. Technol.* **6** (1986) 285.
6. *Idem, Wear*, in press.
7. *Idem, ibid.* **114** (1987) 223.

Received 1 December 1987
and accepted 29 April 1988